Nuclear Materials and Energy 15 (2018) 244–248

Contents lists available at ScienceDirect

Nuclear Materials and Energy

journal homepage: www.elsevier.com/locate/nme

Iron NRT- and arc-displacement cross sections and their covariances

S.P. Simakov[a,*], U. Fischer[a], A.J. Koning[b], A.Yu. Konobeyev[a], D.A. Rochman[c]

[a] Institute for Neutron Physics and Reactor Technology, Karlsruhe Institute of Technology, Eggenstein-Leopoldshafen, 76344, Germany
[b] Nuclear Data Section, International Atomic Energy Agency, Vienna 1400, Austria
[c] Reactor Physics and Systems Behaviour Laboratory, Paul Scherrer Institute, Villigen, 5232, Switzerland

ARTICLE INFO

Keywords:
Iron
Neutron induced damage
Nuclear reaction data
Primary defects
Covariance

ABSTRACT

Displacement damage cross sections have been calculated for natural iron and its constituent individual isotopes based on the latest versions of the evaluated neutron data libraries ENDF/B-VIII.0 and TENDL-2017 using the conventional *NRT* and recently introduced athermal recombination-corrected (*arc)* displacement concepts. Their covariance matrices, which quantify the uncertainties and the associated energy-energy correlations, were assessed for the first time based on TENDL-2017 random data files representing the covariances of the underlying nuclear data. In addition to the nuclear data, the covariances due to the ion energy partition, the primary defect survival efficiency and the lattice threshold energy were also propagated to the damage quantities. The *arc*-dpa was computed employing all available results from molecular dynamics and binary collision simulations. The comparison of the spectrum-averaged *arc*-dpa with the few available measurements at fission reactors has demonstrated a reasonable agreement within the experimental and calculation uncertainties. The comparison with the current *NRT*-dpa standard, provided by ASTM up to 20 MeV but without uncertainty, has indicated differences up to 8% above 0.5 keV and 60% below.

1. Introduction

The *NRT* concept of displacement damage cross section (dpa – displacements per atom), proposed by Norgett et al. [1], provides a basis for the quantification of neutron and ion induced radiation effects in materials. It is also can be used as a scaling factor for the comparison and extrapolation of radiation databases accumulated at existing nuclear facilities to projected ones. Recently a new damage concept based on "athermal recombination-corrected (*arc*) dpa", has been proposed by the OECD Primary Radiation Group [2] and has been adopted for the calculation of damage cross section data by the IAEA Coordinate Research Project on Radiation Damage [3]. *Arc*-dpa quantify the total number of primary lattice defects (i.e., the vacancy-interstitial pairs denoted as Frenkel pairs) which survive after annealing of the hot recoil cascade during the first 10–100 ps after initiation of the nuclear reaction.

The present work provides evaluations of *NRT*- and *arc*-dpa cross sections for the naturally occurring isotopes of iron and elemental iron based on the latest evaluated neutron cross section data files up to 200 MeV. Initial comparative studies of the *NRT*- and *arc*-dpa cross sections and spectrally averaged values for fission, fusion and material testing facilities were carried out but involved only lower energies and used the neutron data available at that time [4–5]. Furthermore, estimates of the dpa covariance matrices (i.e. the uncertainties and associated energy-energy correlations) are provided for the first time as resulting from the involved nuclear data and material physics modelling. This work is an extension of our previous study on the iron main isotope ^{56}Fe [6], covering now the covariance determination for the displacement damage in natural iron.

2. Methods used to compute *NRT*- and *arc*-dpa and their covariances

2.1. Definitions and computing of the damage energy and displacement cross sections

The damage energy *DE* at neutron energy *E* which will be transferred to atoms displaced from their lattice sites in metal can be computed either in the frame of the conventional *NRT* or the new *arc* concepts according to the formulations given, e.g. in [1,2,7]. Since we used the NJOY code to compute *DE*, only a simplified formula is given here to show the variables which we derived or sampled but omitting others such as integration over scattering angle etc.:

* Corresponding author.
E-mail address: stanislav.simakov@kit.edu (S.P. Simakov).

https://doi.org/10.1016/j.nme.2018.05.006
Received 15 December 2017; Received in revised form 11 May 2018; Accepted 13 May 2018
Available online 24 May 2018

$$DE_{NRT} = \sum_{j,i} \int_{E_d}^{\infty} \frac{d\sigma_j(E, T_i)}{dT_i} \widehat{T_i}\, dT_i \quad DE_{arc}$$
$$= \sum_{j,i} \int_{E_d}^{\infty} \nu(T_i) \frac{d\sigma_j(E, T_i)}{dT_i} \widehat{T_i}\, dT_i \;\; where \;\; \widehat{T_i}$$
$$= \begin{cases} 0, & 0 < P(T_i)T_i < E_d \\ \frac{2E_d}{0.8}, & E_d < P(T_i)T_i < 2E_d/0.8 \\ P(T_i)T_i, & \frac{2E_d}{0.8} < P(T_i)T_i < \infty \end{cases} \quad (1)$$

In Eq. (1), $d\sigma_j(E,T_i)/dT_i$ is the energy differential cross section for the production of primary knock-on atoms (PKA) or charged particles i with kinetic energy T_i for the neutron-induced reaction channel j; $P(T_i)$ - the ion energy partition function (i.e., the fraction of recoil energy that becomes available for damage) [1,7]; $\nu(T_i)$ – primary defects survival efficiency or fraction of Frenkel pairs (FP) left after athermal cascade annealing phase; E_d – lattice threshold energy or averaged minimum energy needed to create one FP.

The latest official version 99 of the nuclear data processing code NJOY-2012 [7], was used to compute the damage energy for each stable iron isotope $^{54,56.57,58}$Fe from the latest versions of the modern nuclear data evaluations ENDF/B-VIII.0 [8] and TENDL-2017 [9].

The NJOY code implements a model for the damage energy that is not consistent with the NRT damage energy definition in Eq. (1) in the interval E_d $E_d < \widehat{T_i} < 2\ E_d/0.8$. In the case of iron this results in an underestimation of the *NRT*- and *dpa*-cross sections by factor of 2.0/0.8 = 2.5 at neutron energy $E \approx E_d$*A/4 = 0.65 keV, where A is atomic mass number. For a rigorous implementation of the *NRT* definition we modified the HEATR module of NJOY as documented in [10].

The corresponding *NRT*- and *arc*-dpa cross sections are then derived according to:

$$\sigma_{NRT-dpa}(E) = \frac{0.8}{2\ E_d} DE_{NRT}(E) \text{ or } \sigma_{arc-dpa}(E) = \frac{0.8}{2\ E_d} DE_{arc}(E) \quad (2)$$

The *DE*- and *dpa*-cross sections for natural iron were produced from isotopic cross sections by the MIXR module of NJOY taking into account the isotope abundances a_n: ^{54}Fe – 5.9%, ^{56}Fe – 91.72%, ^{57}Fe – 2.1%, ^{58}Fe – 0.28%.

In the present work the uncertainties and energy-energy correlations of *DE(E)* or *σ-dpa(E)* were computed independently from the different underling data or models, namely from: nuclear data, PKA energy partition function, FP survival efficiency and Ed. It means when one component was randomized, the others were used unperturbed.

2.2. Computation of the damage cross section covariances from TENDL-2017 evaluated neutron data files

The covariance matrix for *DE*- and *dpa*-cross sections were computed from five hundred TENDL-2017 random files which were generated by the Bayesian Monte Carlo method (i.e. by sampling and assigning the proper weights for the input parameters of the underlying nuclear reaction models) [9]. Each of these 500 random files were also processed by the NJOY code and additionally grouped into 228 energy bins to reduce the rank of covariance matrices but still retaining a rather detailed energy representation of cross sections. The energy group structure of VITAMIN-J 175 was chosen, which covers the energies from 10^{-5} eV to 19.64 MeV, plus 1 – 2 MeV wide bins up to 200 MeV.

The first order covariance matrix for values y_i (i.e., either $DE(E_i)$ or σ-$dpa(E_i)$) in every bin i was calculated from the N_{random} ensemble following the general definitions [11]:

$$cov(y_i, y_j) = \sum_{k=1}^{Nrandom} \frac{(y_i^k - \bar{y}_i)\left(y_j^k - \bar{y}_j\right)}{N_{random}}, \quad (3)$$

where indices i or j refer to the k random value of quantity y_i^k in the specific energy groups and $\bar{y}_i$ is an averaged value. The diagonal elements ($i = j$) of the covariance matrix provide the variance or square of the standard deviation σ_i:

$$\sigma_i^2 = cov(y_i, y_i) \quad (4)$$

The energy-energy correlation matrix was then calculated as:

$$cor(y_i, y_j) = \frac{cov(y_i, y_j)}{\sigma_i \sigma_j}, \quad cor(y_i, y_i) = 1 \quad (5)$$

The covariances matrices were firstly computed for each isotope ^{54,56,57,58}Fe from the corresponding isotopic TENDL-2017 random files. Then the covariance matrix for natural iron was obtained by summing up the variances of the individual isotopes taking into account the iron isotope abundancies a_n and absence of the cross isotope correlations in the TENDL-2017 random evaluation:

$$cov_{nat}(E_i, E_j) = \sum_{n=1}^{4} a_n^{2} * cov_n(E_i, E_j) \quad (6)$$

For illustration, the results of the calculation of the *NRT* damage energy and its uncertainties resulting from the nuclear data for natural iron and two isotopes ^{54,56}Fe are shown in Fig. 1. It is interesting to note that ^{56}Fe gives a dominant contribution to the *DE* cross section and the uncertainty at all energies except in the vicinity of 8 keV where the n - ^{54}Fe resonance prevails over ^{56}Fe. The energy-energy correlation matrix derived from TENDL-2017 neutron random files shows two energy

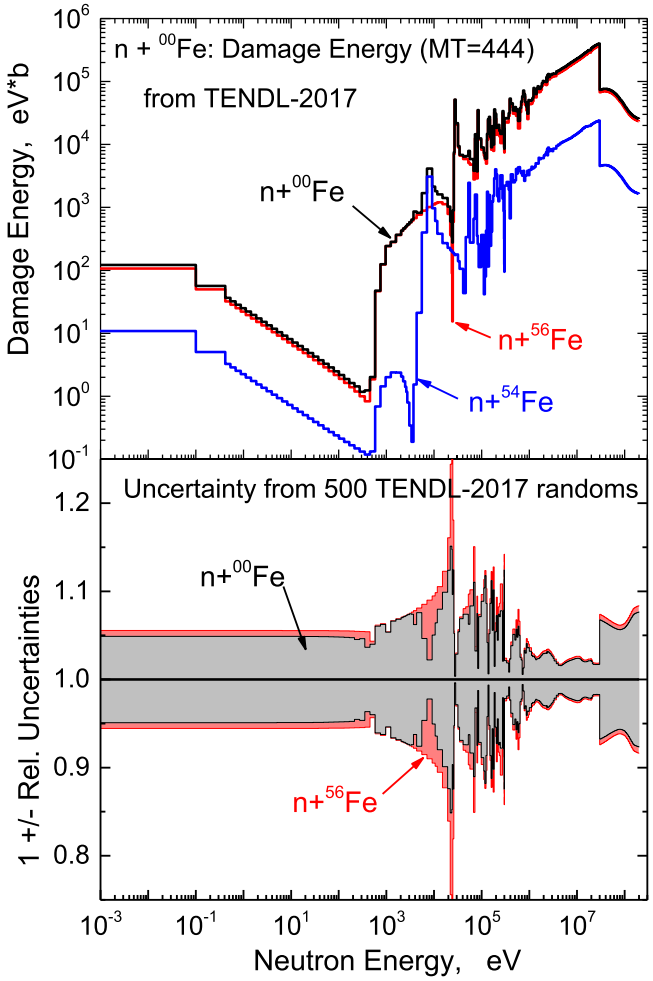

Fig. 1. The NRT damage energy (top) and uncertainty (bottom) derived from TENDL-2017 random files for natural iron. The contributions from ^{56}Fe and ^{54}Fe are depicted by colour curves.

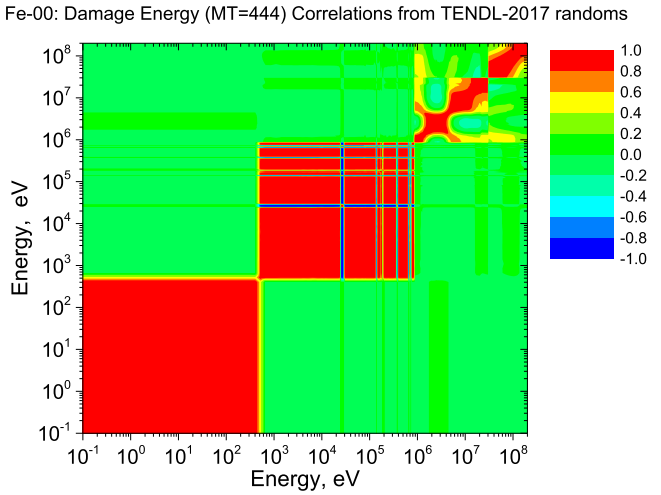

Fig. 2. The energy-energy correlation matrix for the NRT damage energy derived from TENDL-2017 random files for natural iron.

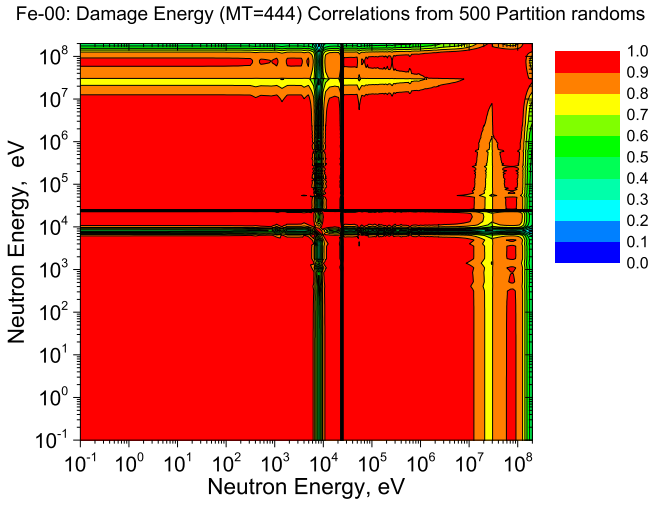

Fig. 3. The energy-energy correlation matrix for the NRT damage energy derived from the variation of parameters of the Fe ions energy portioning in natural Iron.

domains of high correlations however without correlation between them, see Fig. 2.

2.3. Covariances due to involved materials physics modelling

In additional to the neutron-nucleus interaction cross section several other phenomena which reflect the material physics have impact on the calculation of the damage energy and the displacement cross sections.

Partitioning of the recoil atom energy between the kinetic energy delivered to the lattice knock-on atoms (real damage energy) and the ion energy losses due to Coulomb interaction with electrons. The most commonly used partition function was introduced by M. Robinson who has fitted J. Lindhard's theory of energy splitting between atomic and electronic motion [12]. The uncertainties of three parameters used in Robinson's formula were derived from the comparison with the spread of the number of NRT defects computed by the IOTA code [13]. Different approximations of the ion-ion scattering cross section were used, which eventually define the nuclear stopping power of ions. During the processing of the non-perturbed TENDL-2017 files by the NJOY code, we varied the parameters of the partition function within ± 12% and generated 500 random damage energy files. Their statistical analysis using Eq. (3) has resulted in the production of the covariance matrices for each Fe isotope. The mixing of four isotopes finally yields the damage energy covariance matrix for natural iron as a result of the partition function. The correlation matrix displayed in Fig. 3 shows strong correlations between practically all neutron energies.

Frenkel pair defect survival efficiency according to Eq. (1) affects only *arc*-dpa, since it depends on $\nu(T)$, but not *NRT*-dpa. The number of FP defects is usually computed by molecular dynamics (MD) simulations which depend on the interatomic potential used. The different potentials as well as statistical uncertainties due to a limited number of simulated tracks result in the variation of MD predictions for the survival efficiency.

Fig. 4 shows the MD results collected in the overview [2] and several additional independent ones [4,14,15] (the results obtained with the use of potentials published in the later paper will appear elsewhere soon) for the PKA energy up to 200 keV – that is sufficient for fission applications. To cover the energy range of recoils produced also in fusion and accelerator driven facilities, the survival efficiency has to be defined up to 1040 keV (fusion, maximum neutron energy 15 MeV) or 3830 keV (International Fusion Material Irradiation Facility IFMIF, maximum neutron energy 55 MeV). These values are the energies of ^{56}Fe recoils emitted in forward direction by elastic neutron scattering on ^{56}Fe (the exothermic ^{56}Fe(n,α) reaction may produce Cr recoils with even higher energies, see Simakov et al. [5]). Since MD simulations are

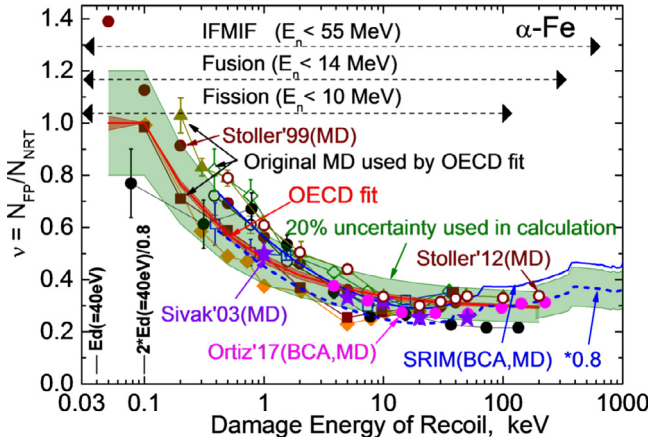

Fig. 4. Frenkel pairs (FP) survival efficiency versus PKA damage energy in pure iron: symbols – results of MD simulations collected in [2], original data from [4,14,15] and BCA-MD from [16,17], red curve – fit recommended by OECD group [2], green band - ± 20% uncertainty assigned to represent the spread and uncertainties of known MD calculations. Dashed horizontal lines with arrows show the PKA damage energies range generated in fission or fusion reactors and IFMIF. (For interpretation of the references to colour in this figure legend, the reader is referred to the web version of this article.)

currently not capable of computing the number of FP at such high recoil energies, the binary collision approach (BCA) or its combination with MD simulations [16,17], is a practical way to estimate the defect survival efficiency - see available computational results in Fig. 4.

In the present calculations we eventually used the defect survival efficiency from the OECD fit [2] up to 200 keV (represented as a table) and the SRIM based MD-BCA results [16] at higher energies, after downscaling by the factor 0.8 to match the OECD fit. The uncertainties assessed in [2] amount only to ± (2–4)% that do not reflect the spread of the MD simulation results as seen in Fig. 4. To capture the latter effect we assigned a ± 20% uncertainty to the survival efficiency.

The recoil energy-energy correlations of the damage efficiency originate from the equations and parameters used in the MD simulations. We did not found in the literature quantitative information which helps us to construct the correlation matrix. On other hand some MD simulations studies, see in [2] and [14], have reported the statistical uncertainty within 10–20% for PKA energies below ≈40 keV. As seen in Fig. 4, the statistical error bars are comparable with spread of

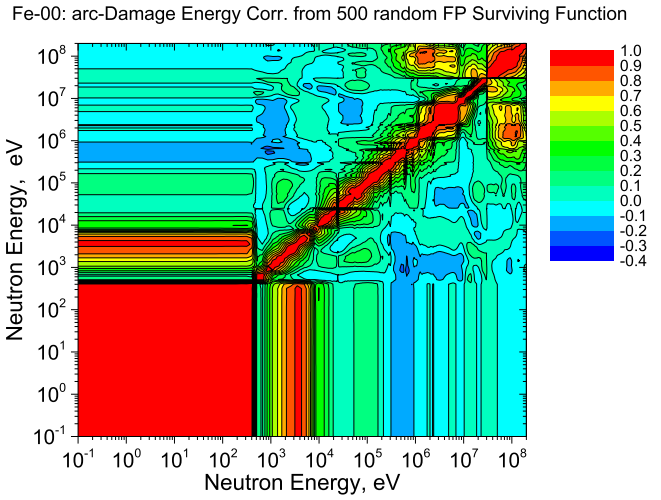

Fig. 5. The energy-energy correlation matrix for the natural iron *arc* damage energy which is caused by the uncertainties of the FP survival efficiency.

individual results. The dominance of the statistical uncertainty below 40 keV means an absence of the energy-energy correlation for the defect survival efficiency. In the present work we accepted such correlation matrix for the whole energies of PKA.

The resultant energy-energy correlation matrix of the *arc* damage energy for elemental iron, which is induced by the uncertainties of the FP survival efficiency, is plotted in Fig. 5. As expected it shows no correlation. Exception is the neutron energies below 0.5 keV, where the (n,γ) reaction dominates in the production of recoils. Due to the kinematics of this reaction even neutrons with different energies up to 50 keV will produce recoils with the same energy, hence the computing of the number of survived defects will involve the equal survival defect efficiency. This results to the full energy-energy correlation matrix for neutrons below 0.5 keV.

Lattice Threshold Energy. K. Nordlund and co-workers have estimated the mean value and uncertainty of threshold energy for iron as $E_d = 40 \pm 2$ eV [18]. Following Eq. (2), this 5% relative uncertainty will directly propagate to the *NRT*- and *arc*-dpa and will imply a 100% correlation for all considered neutron energies.

The E_d uncertainty will additionally impact on the damage energy *DE* since it defines the lowest energy limit of PKA integration in formula (1). It is clear that this threshold effect will manifest itself in the narrow neutron energy interval 500 −1000 eV.

3. Discussion and comparison with experiments

Fig. 6 shows the *NRT*-dpa cross section for natural iron up to 200 MeV, derived from the latest evaluated neutron cross section libraries ENDF/B-VIII.0 and TENDL-2017 and the *arc*-dpa cross section, which additionally take into account the Frenkel pair survival efficiency from available MD and BCA-MD simulations.

For the first time the total uncertainty and energy-energy correlation for radiation damage quantities, as well as the partial contributions from used physical models, were estimated on the basis of the assumptions used here. As seen in the bottom of Fig. 6, the nuclear data lead to (5 – 10)% uncertainties and strong positive energy-energy correlations within 2 large regions not correlating to each other (Fig. 2); ion energy partition – (2 – 5)% uncertainties and strong positive E-E correlations (Fig. 3); defect survival efficiency – (5 - 15)% and non-correlation except the energy range where (n,γ) reaction dominates (Fig. 5), lattice threshold – 5% uncertainty and full E-E correlation.

The *NRT*- and *arc*-dpa cross section derived from TENDL-2017 random files drop off at 30 MeV. The reason was found to be an improper storage of relevant nuclear reaction data in the formatted files

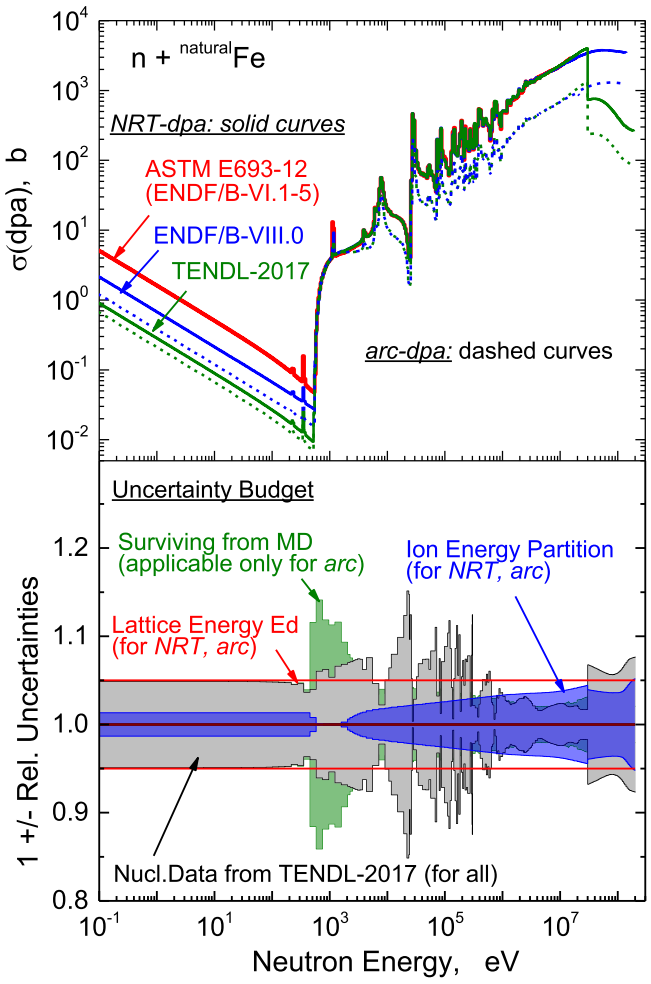

Fig. 6. *NRT*- and *arc*-dpa cross section (top) and uncertainty (bottom) with contribution from nuclear data, ion energy partition, FP defect surviving efficiency and lattice threshold for natural iron. For comparison the ASTM E693 *NRT* standard for iron is shown.

that will be corrected in the next TENDL release. Due to this reason the nuclear data uncertainties and energy-energy correlations calculated from the TENDL-2017 random files above 30 MeV are not representative and will be reassessed after release of the corrected TENDL version.

For comparison the ASTM E693-12 standard [19], which is an actual *NRT* reference for iron up to 20 MeV neutron energy, is also plotted in Fig. 6. It has to be noted that this standard was computed from the evaluated neutron cross sections library ENDF/B-VI which is nowadays obsolete. To show a difference resulting from the evolution of the ENDF library, the ratio of ASTM E693-12 to the ENDF/B-VIII.0 *NRT*-dpa cross section is plotted in Fig. 7: ASTM is 2 times higher below neutron energy 0.5 keV and deviates up to 8% at higher energies. The rather large difference at lowest energies is not a result of the change of the Fe neutron capture cross section, but comes from the damage energy computed by NJOY. However, as it was shown many times for fission and fusion applications, the neutrons with energies less than 100 keV do not typically contribute significantly to the total dpa fluence.

The *arc*-dpa cross section, as seen in Figs. 6 and 7, is less than the *NRT*-dpa by factor 2 - 3 except for the neutron energies from 0.57 to 2–3 keV. The latter interval corresponds to PKA recoils where the FP survival efficiency is close to unity.

The *NRT*-dpa cross section can not be compared with experimental data and thus be validated since it is practically a non observable physical quantity. However an estimate of the *arc*-dpa for Fe can be

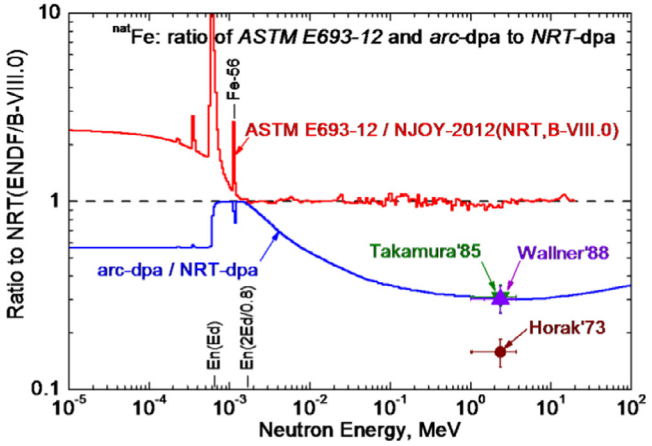

Fig. 7. Ratio of the ASTM E693-12 standard for iron to *NRT*-dpa cross section derived by NJOY-2012.99 from ENDF/B-VIII.0 (red curve). Ratio of *arc*-dpa and *NRT*-dpa cross sections: computed in the present work (blue curve) and obtained from measurements of Horak and Blewitt [20], Takamura and Aruba [21] and Wallner et al. [22] (symbols). (For interpretation of the references to colour in this figure legend, the reader is referred to the web version of this article.)

Table 1
Comparison of computed *arc*-dpa cross section averaged in a $^{235}U(n_{th},f)$ prompt fission spectrum with measurements carried out in fast fission fields at cryogenic temperature.

Existing measurements at ≈4.5 °K	Computed in $^{235}U(n_{th},f)$ PFNS [23]
Horak'76 [20] = 136 ± 23 b Takamura'86 [21] = 264 ± 44 b Wallner'88 [22] = 260 ± 43 b	*arc-dpa* = 261 ± 26 b *dpa* = *841* ± *(for comp:. NRT-dpa = 841 ± 67 b)*

obtained in the experiments where the samples were irradiated at temperature below 10 °K thus preventing the diffusion and annealing of primarily created Frenkel pairs [20,21,22]. The measurements were carried in fast fission neutron spectra, and the number of defects was derived from the change of electrical resistivity. To perform a comparison we have folded the computed *arc*-dpa cross section with the prompt fission neutron spectrum (PFNS) well known for the thermal neutron induced fission of ^{235}U [23]. The results listed in Table 1 and plotted in Fig. 7 show reasonable agreement with two of three existing experiments. The spectrum weighted *NRT*-dpa given there for comparison is 3.2 times larger than *arc*-dpa.

4. Summary

NRT- and *arc*- damage energy and displacement cross sections were computed for individual iron isotopes and natural iron at neutron energies from thermal to 200 MeV employing neutron induced cross sections from the latest nuclear data libraries ENDF/B-VIII.0 and TENDL-2017.

The comparison of the ENDF/B-VIII.0 *NRT*-dpa with the actual standard ASTM E693-12 available up to 20 MeV has shown an agreement within 8% except for energies below 0.5 keV where the lower Fe (n,γ) damage energy cross sections is a result of the NJOY processing of the latest version of the ENDF library. TENDL-2017 gives even lower *NRT*-dpa cross sections below 0.5 keV and additionally exhibits a discontinuity at 30 MeV.

The *arc*-dpa was calculated taking into account available MD and BCA-MD simulations of the number of Frenkel pairs surviving at the end of the ballistic cascade relaxation.

For the first time, the full uncertainty and the associated energy-energy correlations from all contributing components were constructed for *NRT*- and *arc*-dpa cross sections: nuclear data as represented by TENDL-2017 random files (5–15%), recoil energy partition function (2–5%), FP survival efficiency (5–15%) and lattice threshold energy (5%). It has to be stressed that the cross sections and covariances obtained from the TENDL-2017 random files are not valid above 30 MeV, where damage energy is systematically too low.

The *arc*-dpa averaged in fast fission neutron spectrum was shown to agree with measurements performed at cryogenic temperature in fission reactors. Neglecting the energy-energy correlation results in the underestimation of spectrum averaged dpa-rate uncertainty in nuclear facilities by a factor 3–4 [6].

Acknowledgement

This work has been carried out within the framework of the EUROfusion Consortium and has received funding from the Euratom research and training programme 2014-2018 under grant agreement no 633053. The views and opinions expressed herein do not necessarily reflect those of the European Commission.

References

[1] M.J. Norgett, M.T. Robinson, I.M. Torrens, A proposed method of calculating displacement dose rates, Nucl. Eng. Des. 33 (1975) 50.
[2] K. Nordlund, A.E. Sand, F. Granberg, S.J. Zinkle, R. Stoller, et al., Primary Radiation Damage in Materials, OECD, Paris, 2015 Report NEA/NSC/DOC(2015)9.
[3] IAEA Coordinated Research Project F44003 "Primary Radiation Damage Cross Sections"; https://www-nds.iaea.org/CRPdpa/.
[4] R.E. Stoller, L.R. Greenwood, Subcascade formation in displacement cascade simulations: implications for fusion reactor materials, J. Nucl. Mater. 271-272 (1999) 57.
[5] S.P. Simakov, A.Yu. Konobeyev, U. Fischer, V. Heinzel, Comparative study of survived displacement damage defects in iron irradiated in IFMIF and fusion power reactors, J. Nucl. Mater. 386–388 (2009) 52.
[6] S.P. Simakov, A. Koning, A.Yu. Konobeyev, Covariances for the ^{56}Fe radiation damage cross sections, EPJ Web Conf. 146 (2017) 02012.
[7] A.C. Kahler, The NJOY Nuclear Data Processing System, version 2012, ed. Los Alamos National Lab, 2015 Report LA-UR-12-27079.
[8] D.A. Brown, M.B. Chadwick, et al., ENDF/B-VIII.0: the 8th major release of the nuclear reaction data library with CIELO-project cross sections, new standards and thermal scattering data", Nucl. Data Sheets 148 (2018) 1.
[9] A.J. Koning, D. Rochman, Modern nuclear data evaluation with the TALYS code system, Nucl. Data Sheets 113 (2012) 2841.
[10] IAEA CRP F44003: Comparison of NRT-dpa cross sections calculated by NJOY-2012.50 with ASTM standard for natFe; https://www-nds.iaea.org/CRPdpa/NJOY-dpa_vs_ASTM693.pdf.
[11] Wolfram MathWorld, web resources: http://mathworld.wolfram.com/Covariance.html.
[12] M.T. Robinson, The energy dependence of neutron radiation damage in solids, in: J.L. Hall, J.H.C. Maples (Eds.), Proc. Conf. on Nuclear Fusion Reactors, British Nuclear Energy Society, London, 1970, p. 364 17-19 Sep 1969 UKAEA Culham.
[13] A.Yu Konobeyev, U. Fischer, S.P. Simakov, Uncertainty Assessment for the Number of Defects Calculated Using the NRT Damage Model, KIT Scientific, Karlsruhe, 2017 Working Papers, No. 70.
[14] R.E. Stoller, Primary radiation damage formation, in: R.J.M. Konings, T.R. Allen, R.E. Stoller, S. Yamanaka (Eds.), Comprehensive Nuclear Materials, Elsevier Ltd, Amsterdam, 2012, p. 293.
[15] A.B. Sivak, V.A. Romanov, V.M. Chernov, Influence of stress fields of dislocations on formation and spatial stability of point defects (elastic dipoles) in V and Fe crystals, J. Nucl. Mater. 323 (2003) 380.
[16] A.Yu. Konobeyev, U. Fischer, Yu.A. Korovin, S.P. Simakov, IOTA-2017: a Code For the Simulation of Ion Transport in Materials, KIT Scientific Working Papers, Karlsruhe, 2017 No. 63.
[17] Ch. Ortiz, private communication.
[18] K. Nordlund, J. Wallenius, L. Malerba, Molecular dynamics simulations of threshold displacement energies in Fe, Nucl. Instr. Meth. B 246 (2005) 32.
[19] ASTM standard E693-12, Standard practice for characterizing neutron exposures in iron and low alloy steels in terms of displacements per atom (DPA), ASTM International, 2012 June www.astm.org.
[20] J.A. Horak, TM. Blewitt, Isochronal recovery of fast neutron irradiated metals, J. Nucl. Mater. 49 (1973) 161.
[21] S. Takamura, T. Aruba, Fission-neutron displacement cross sections in metals, J. Nucl. Mater. 136 (1985) 159.
[22] G. Wallner, M.S. Anand, L.R. Greenwood, M.A. Kirk, W. Mansel, W. Waschkowski, Defect production rates in metals by reactor neutron irradiation at 4.6K, J. Nucl. Mater. 152 (1988) 146.
[23] A. Trkov, R. Capote, Evaluation of the prompt fission neutron spectrum of thermal-neutron induced fission in U-235, Phys. Procedia 64 (2015) 48.